



RESEARCH ARTICLE

10.1002/2015GC005819

Effects of chemical composition, water and temperature on physical properties of continental crust

Mattia Guerri¹, Fabio Cammarano¹, and James A. D. Connolly²¹Section of Geology, Department of Geosciences and Natural Resource Management, University of Copenhagen, Denmark, ²Earth Sciences Department, Swiss Federal Institute of Technology, Zurich, Switzerland

Key Points:

- Proposed continental crust compositions result in different physical properties
- Phase reactions may cause crustal seismic discontinuities
- Inferring composition from geophysical data requires thermodynamic constraints

Supporting Information:

- Supporting Information S1

Correspondence to:

M. Guerri,
mattia.guerri@ign.ku.dk

Citation:

Guerri, M., F. Cammarano, and J. A. D. Connolly (2015), Effects of chemical composition, water and temperature on physical properties of continental crust, *Geochem. Geophys. Geosyst.*, 16, doi:10.1002/2015GC005819.

Received 18 MAR 2015

Accepted 6 JUL 2015

Accepted article online 14 JUL 2015

Abstract We explore the influence of major elements chemistry and H₂O-content on the density and seismic velocity of crustal rocks by computing stable and metastable crustal mineralogy and elastic properties as a function of pressure and temperature (P-T). Proposed average compositions of continental crust result in significantly different properties, for example a difference in computed density of ~ 4 % is obtained at a given P-T. Phase transformations affect crustal properties at the point that crustal seismic discontinuities can be explained with mineral reactions rather than chemical stratification. H₂O, even if introduced in small amount in the chemical system, has an effect on physical properties comparable to that attributed to variations in major elements composition. Thermodynamical relationships between physical properties differ significantly from commonly used empirical relationships. Density models obtained by inverting CRUST 1.0 compressional wave velocity are different from CRUST 1.0 density and translate into variations in isostatic topography and gravitational field that ranges ±600 m and ±150 mGal respectively. Inferred temperatures are higher than reference geotherms in the upper crust and in the deeper portions of thick orogenic crust, consistently with presence of metastable rocks. Our results highlight interconnections/dependencies among chemistry, pressure, temperature, seismic velocities and density that need to be addressed to better understand the crustal thermo-chemical state.

1. Introduction

Knowledge of the thermal and compositional structure of the Earth's crust is fundamental to understanding the processes that formed the crust and determine its evolution. To constrain the crustal thermal and compositional state it is necessary to compile its physical properties. Correcting for the effects of the crust is also crucial in studies targeting the seismic and density structure of the mantle [e.g., Ritsema *et al.*, 2009; Tondi *et al.*, 2012].

Various crustal models have been proposed in literature, both at a local [e.g., Molinari and Morelli, 2011; Baranov, 2010] and global scale [e.g., Nataf and Richard, 1996; Meier *et al.*, 2007; Shapiro and Ritzwoller, 2002; Laske *et al.*, 2013]. These models mostly rely on observations of compressional wave velocities or on surface waves. Other physical properties are usually inferred with empirical relationships, like those presented in Ludwig *et al.* [1970], Christensen and Mooney [1995] and Brocher [2005].

Brocher [2005] provides relations between compressional and shear wave velocities (V_p and V_s) and between V_p and density that have been widely used by the scientific community [e.g., Molinari and Morelli, 2011; Laske *et al.*, 2013]. Brocher [2005] relations are based on various sources, i.e., borehole data, laboratory experiments, field measurements and estimates from seismic tomography studies. Laboratory measurements consist of experiments on different types of sedimentary, metamorphic and igneous rocks. For crystalline rocks, the main reference is Christensen [1996], a compilation of, primarily, ambient temperature and moderate pressure (< 1GPa) experimental results.

The chemical composition of the continental crust is a long-standing problem in Earth science and has been the target of scientific investigation for decades [Clarke, 1889; Goldschmidt, 1933; Taylor and McLennan, 1985; Rudnick and Gao, 2003]. Our knowledge is limited by various factors, such as the lack of data in remote areas (Antarctica, Siberia, northern part of North-America, etc.), strong lateral heterogeneities and non-uniqueness in the relations between observable physical properties (such as seismic velocities) and chemical compositions. Indeed, rocks with similar V_p can be petrologically and chemically different [Christensen and Mooney, 1995].

Table 1. Tested Chemical Compositions^a

	Upper Crust (wt. %)			Middle Crust (wt. %)			Lower Crust (wt. %)		
	RG	SH	TM	RG	SH	TM	RG	SH	TM
Na ₂ O	3.27	3.56	3.89	3.39	3.55	3.89	2.65	2.70	2.79
MgO	2.48	2.30	2.20	3.59	1.27	2.20	7.24	4.36	6.28
Al ₂ O ₃	15.4	15.05	15.05	15.00	16.21	15.05	16.90	17.40	16.10
SiO ₂	66.62	66.8	65.89	63.50	69.40	65.89	53.40	58.30	54.30
K ₂ O	2.80	3.19	3.39	2.30	3.36	3.39	0.61	1.47	0.64
CaO	3.59	4.24	4.19	5.25	2.96	4.19	9.59	7.68	8.48
FeO	5.04	4.09	4.49	6.02	2.72	4.49	8.57	7.09	10.06

^aRG [Rudnick and Gao, 2003], SH [Shaw et al., 1986]; TM [Taylor and McLennan 1985, 1995].

Geophysical observations, spanning seismic, gravity and magnetotelluric data [e.g., Dong et al., 2014; van der Meijde et al., 2015; Yousof et al., 2013], provide a wide range of constraints on structure and physical properties of the crust. For example, satellite gravity measurements provide constraints even in remote areas where seismic data are missing [Reguzzoni and Sampietro, 2015]. To take advantage of these observations, and to interpret them in terms of crustal thermo-chemical structure, it is necessary to have robust relations between physical properties, chemical composition and temperature.

The aim of this work is to explore how variations in chemical composition and temperature affect the physical properties of crustal rocks. We use phase equilibrium models [Connolly, 2009], based on thermodynamic data [Hacker and Abers, 2004; Holland and Powell, 1998; Jagoutz and Behn, 2013] to obtain relationships between seismic velocities and density as a function of pressure, temperature and composition. We consider three compositional models proposed for the continental crust [Rudnick and Gao, 2003; Shaw et al., 1986; Taylor and McLennan, 1995, hereafter RG, SH, TM, oxides content in Table 1]. The compositions given in these models are anhydrous. We add different amounts of H₂O to each composition to test the effect of H₂O content on physical properties. Crustal lithologies may persist metastably, particularly at low temperature due to kinetic factors. To account for this effect we also compute physical properties by considering reference mineralogies for upper, middle and lower crust. In this case the metastable mineralogies remain constant, but the physical properties vary as function of pressure and temperature.

We use our computed relations between seismic velocity and density to build models for the physical properties of the crystalline layers of the continental crust. We apply our relationships to: (i) determine temperatures, density and V_S by inverting V_P data from CRUST 1.0 (CR1) [Laske et al., 2013] and (ii) infer density and seismic velocities using a thermal structure based on heat-flow constraints [Davies, 2013]. To constrain pressure, we assume the depth and thickness of the crystalline layers given in CR1 in both cases. The obtained models are compared with CR1. The comparison does not aim to identify which of them better fits CR1, rather we aim to quantitatively investigate the discrepancies between physical properties inferred with our thermodynamically based relations versus properties obtained with empirical relations. We also explore how variations in density distribution between the models affect isostatic topography and the gravitational field.

2. Methodology

2.1. Crustal Composition and Calculation of Physical Properties

Previous authors have used a multidisciplinary approach to infer crustal chemical composition, involving for example (i) surface exposure studies, (ii) borehole data, (iii) interpretation of seismic velocities in terms of petrology relying on laboratory experiments, (iv) analysis of xenoliths and xenocrysts, (v) surface heat flow data [Rudnick and Gao, 2003]. Various average anhydrous compositions for the continental crust have been proposed (see Rudnick and Gao [2003] for a review on this topic). We choose TM and SH because they represent extremes in terms of silica content. In addition, we consider the most recent RG, which has an intermediate SiO₂ content. Three different averages for upper middle and lower crust, respectively, are given for both RG and SH. These compilations are therefore coherent with the CR1 model, in which the crystalline crust is subdivided in three layers. TM consists of only two averages, one for the upper crust and the other one for the lower crust. In this case we assign to the middle crust the same composition of the lower crust. To investigate the influence of H₂O on crustal physical properties, we test two variants on each of the

aforementioned compositions by adding 0.25 and 0.50 wt. % of H₂O. Hydrated compositions are named by adding 025 or 050 after the used acronym for dry compositions. RG025, for example, refers to RG composition with 0.25 wt. % of H₂O added.

We compute stable mineralogy as a function of P-T for each composition by free energy minimization [Connolly, 2009] with the thermodynamic data from Holland and Powell [1998] augmented with elastic moduli from Hacker and Abers [2004] and Jagoutz and Behn [2013], permitting the computation of seismic wave speeds. The crust is modeled in the Na₂O-CaO-K₂O-FeO-MgO-Al₂O₃-SiO₂-H₂O system. The chosen solution models and related references are given in the supporting information Table S1. Aggregate bulk and shear moduli are computed by Voigt-Reuss-Hill averaging of the moduli of the constituent minerals [Bina and Helffrich, 1992]. V_p and V_s for the bulk rock are then obtained as:

$$V_p = \left(\frac{k + 4/3 \mu}{\rho} \right)^{1/2} \quad (1)$$

$$V_s = \left(\frac{\mu}{\rho} \right)^{1/2} \quad (2)$$

The estimated error in the computed seismic velocities for the single mineral is < 2% [Hacker et al., 2003]. The main shortcomings of computing V_p and V_s in this way are that no account is made for the effects of anisotropy, anelasticity and porosity. Anisotropy in the crust is related to a variety of mechanisms, i.e., layering, parallel-aligned major structural elements (faults and fractures), parallel-aligned microcracks and crystal preferred orientation of anisotropic minerals. Anisotropy is a poorly constrained factor on a global scale and therefore we do not attempt to model it. Anelasticity could play an important role at high temperatures, leading to an increase of sensitivity of V_s and V_p variations to temperature in hot regions [Karato, 1993; Cammarano et al., 2003]. In the crust, the presence of pores filled by fluids has been also associated with mechanisms of seismic attenuation [Sato et al., 2012]. Modeling anelasticity in the crust is a challenging task since most of the seismic attenuation is due to scattering and not to intrinsic factors. However, at a global scale, to a first approximation it is reasonable to neglect anelasticity. Porosity, including fractures, is particularly important in the upper crust. Experimental tests show that voids are closed at pressure larger than 250 MPa [Kern, 1990], unless fluids fill the voids. We test porosity effects on our results by applying empirical laws to model its depth variation [Vitovtova et al., 2014] and influence on compressional wave velocities [Wyllie et al., 1958].

2.2. Crustal Models Computation

Among the various global models of crustal properties and structure that have been proposed in the literature, CR1 and its older versions, CRUST 5.1 and CRUST 2.0, are the only models that present values of both compressional and shear waves velocity together with density. CR1 is based on active source seismic studies and receiver functions. Gravity data are used where seismic constraints are missing and 19 crustal types are assumed (Figure 1, only principal nine continental crustal types are shown) according to basement age and tectonic settings (a complete list of the crustal types and their physical properties is available at <http://igppweb.ucsd.edu/~gabi/rem.html>). The scaling between V_p , V_s and density has been validated against the empirical relations by Brocher [2005].

In this study, we use thermodynamically constrained relationships to compute models of physical properties for the crustal crystalline layers. We follow two approaches. In one, we invert CR1 V_p data (model downloaded at igppweb.ucsd.edu/~gabi/crust1.html, data accessed 31 October the 2013) in the upper, middle and lower crust for temperatures, V_s and density, obtaining a series of models that we call "inverted models." In our second approach, we compute crustal physical properties for the same layers through thermodynamic modeling and considering the thermal structure obtained as described in section 2.3. This procedure results in models that we refer to as "forward models." These approaches are detailed in the following two sections.

2.2.1. Inverted Models

The data on which CR1 primarily relies are V_p measurements from seismic refraction studies. We invert CR1 V_p in temperature, V_s and density, through the following procedure (we refer to the obtained models as "equilibrium inverted models"):

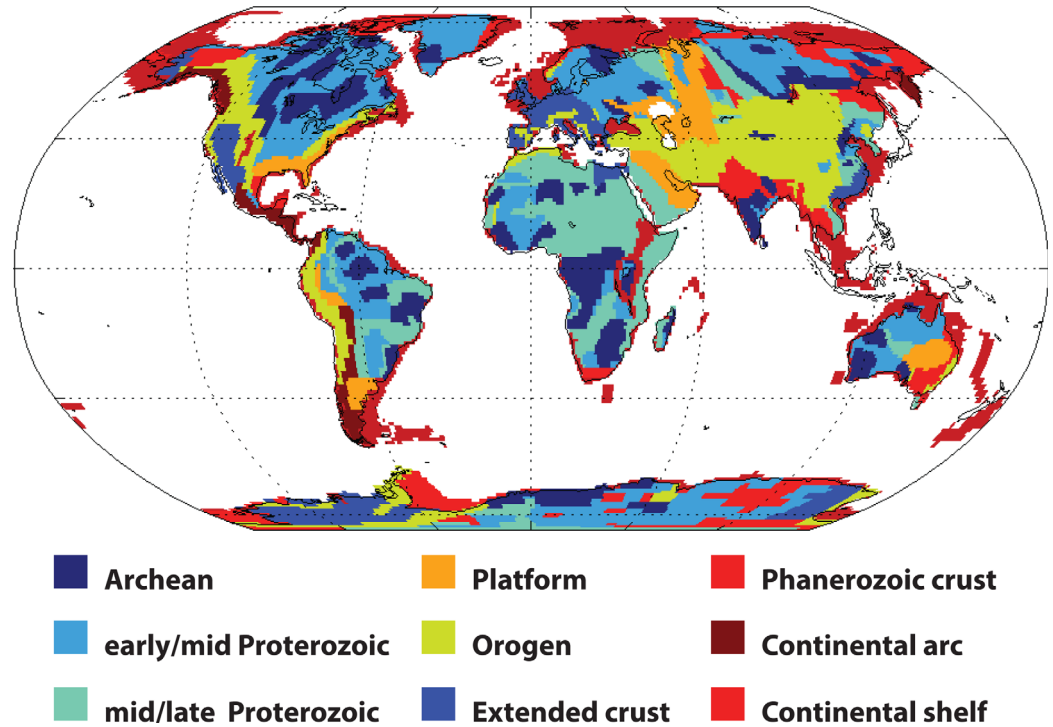


Figure 1. Continental crustal types in which the model CR1 [Laske et al., 2013] is subdivided.

1. Compute V_p , V_s and density tables. For each composition, we compute stable mineralogy, V_p , V_s and density by phase equilibrium modeling at increments of 1 MPa in pressure and 10 K in temperature.
2. Discretize CR1 depths and assign pressure values. CR1 gives thickness and average physical properties of each layer. For each latitude-longitude cell, we discretize the CR1 vertical parameterization by steps of 100 m. We then compute for each depth node an associated pressure value given the density of the overlying rocks.
3. Invert CR1 V_p values for V_s , temperature and density. At this point, we have a V_p value and a pressure value at each CR1 node. We search our precomputed tables for a V_p -pressure value that matches the CR1 value. The thermodynamically modeled V_p is associated with values of temperature, V_s and density that represent our inverted physical properties. Pressure is recomputed again considering the obtained density structure, and the inverted parameters are perturbed according to the new pressure. We iterate until density converges [Cammarano, 2013].
4. Average over each layer. To obtain models comparable with CR1, we average with depth the physical properties of the inverted models in each layer.

To simulate metastable conditions, we compute another series of inverted models referred to as "metastable inverted models." These are obtained with the same procedure as described above but instead of relying on equilibrium mineralogies, they are based on the reference mineralogies showed in Table 2. The reference mineralogies correspond to the stable mineralogies obtained by phase equilibrium calculations at P-T conditions taken to be representative of the upper, middle and lower crust, 165.9 MPa–467 K, 495.8 MPa–709 K, 819.9 MPa–906 K. The mineralogies are metastable at any P-T condition other than that at which they were computed.

We identify the "equilibrium inverted models" with four letters and, in case of wet compositions, three numbers. For example, the models EIRG and EIRG025 are inverted models obtained with the compositions RG and RG025, respectively. The same system of abbreviation is used for the "metastable inverted models," e.g., MIRG and MIRG025 are models computed with metastable mineralogies using RG and RG025 composition.

Table 2. Reference Mineralogies Used for Metastable Models Computation

Phase	wt. %	Na ₂ O	MgO	Al ₂ O ₃	SiO ₂	K ₂ O	CaO	FeO	
Upper Crust (RG Composition) Stable Phases at 165.9 MPa–467 K									
Orthopyroxene	15.59		0.93		2.00			1.06	
Feldspar (Sanidine)	16.93	0.01		0.50	3.00	0.49			
Feldspar (Anorthite)	11.70	0.01		1.00	2.02		0.98		
Feldspar (Plagioclase)	33.89	0.41		0.59	2.82		0.18		
Kyanite	0.69			1.00	1.00				
Quartz	21.19				1.00				
Middle Crust (RG Composition) Stable Phases at 495.8 MPa–709 K									
Orthopyroxene	17.37		0.96	0.02	1.98			1.04	
Feldspar (Sanidine)	14.26	0.033		0.50	3.00	0.47			
Feldspar (Plagioclase)	46.11	0.31		0.69	2.63		0.37		
Omphacite	6.93	0.01	0.66	0.10	1.92		0.97	0.23	
Quartz	15.33				1.00				
Lower Crust (RG Composition) Stable Phases at 819.9 MPa–906 K									
Orthopyroxene	28.13		1.09	0.054	1.95			0.85	
Feldspar (Sanidine)	2.59	0.05		0.51	3.00	0.44	0.02		
Feldspar (Plagioclase)	50.87	0.22		0.77	2.47	0.01	0.53		
Omphacite	16.78	0.02	0.62	0.16	1.85		0.96	0.20	
Quartz	1.64				1.00				
Phase	wt. %	H ₂ O	MgO	Al ₂ O ₃	SiO ₂	K ₂ O	CaO	FeO	Na ₂ O
Upper Crust (RG025 Composition) Stable Phases at 165.9 MPa–467 K									
Orthopyroxene	10.01		0.93		2.00			1.06	
Amphibole (Glaucophane)	7.30	1.00	0.96	1.02	7.96		0.04	2.04	0.98
Amphibole	4.71	1.00	2.59	1.50	6.00		2.00	1.41	0.50
Feldspar (Sanidine)	16.90			0.50	3.00	0.49			0.01
Feldspar (Anorthite)	9.95			0.99	2.02		0.98		0.01
Feldspar (Plagioclase)	26.63			0.59	2.82		0.18		0.41
Kyanite	1.57			1.00	1.00				
Quartz	22.94				1.00				
Middle Crust (RG025 Composition) Stable Phases at 495.8 MPa–709 K									
Orthopyroxene	12.50		0.89	0.02	1.98			1.09	
Amphibole	12.39	1.00	2.39	1.44	6.08		1.99	1.64	0.48
Feldspar (Sanidine)	14.29			0.50	3.00	0.46			0.03
Feldspar (Plagioclase)	39.29			0.68	2.64		0.36		0.32
Omphacite	3.18		0.62	0.10	1.92		0.97	0.26	0.01
Quartz	18.35				1.00				
Lower Crust (RG025 Composition) Stable Phases at 819.9 MPa–906 K									
Orthopyroxene	23.37		1.06	0.06	1.94			0.88	
Amphibole	12.21	1.00	2.84	1.22	6.38		1.98	1.33	0.41
Feldspar (Sanidine)	2.77			0.51	2.99	0.44	0.01		0.05
Feldspar (Plagioclase)	45.66			0.77	2.45	0.01	0.55		0.21
Omphacite	12.06		0.60	0.16	1.85		0.97	0.21	0.02
Quartz	3.93				1.00				

2.2.2. Forward Models

Vast areas of the continental crust (South America, northern North America, Siberia, Australia, Antarctica) are not covered by the seismic data upon which CR1 relies. We therefore attempt a forward calculation of physical properties of the continental crust on a global scale. We consider the pressure values estimated from CR1 layers thicknesses and we rely on independent estimates of temperatures obtained as described in section 2.3. The procedure to compute the forward models involves the same first two steps as the procedure for the inverted models and the following additional steps:

3. *Determine V_p , V_s and density at a given P-T.* For each composition, we extract from the precomputed thermodynamical tables, V_p , V_s and density associated with estimated temperature at each node. The conversion from depth to pressure is carried out by the iterative method outlined in step 3 of previous section.
4. *Average over each layer.* The new physical properties models are averaged with depth in each layer, to make them comparable with CR1.

As in the case of the inverted models, in the forward models we carry out computations both at thermodynamic equilibrium and considering the reference mineralogies reported in Table 2. Forward models are identified similarly to the inverted models. For example, EFRG and EFRG025 are models computed, respectively, with RG and RG025 composition at thermodynamic equilibrium.

2.3. Thermal Structure of the Continental Crust

We obtain a reference thermal model for the continental crust on the basis of *Davies* [2013] global map of surface heat flow. The map is parameterized on a 2° equal area grid and it is based on more than 38,000 measurements. In areas where no heat-flow data are available, a correlation between heat flow and surface geology is assumed, assigning the same heat-flow value of a geologically similar region.

We compute geotherms using the solution of the one-dimensional steady state conductive heat transfer equation [*Chapman*, 1986]:

$$T(z) = T_0 + \frac{q_0}{k}z - \frac{Az^2}{2k} \quad (3)$$

where T_0 is surface temperature, q_0 is surface heat flow, k is thermal conductivity, A is volumetric heat production and z is depth. For a layer of thickness Δz , with constant heat generation and thermal conductivity, temperature T_B and heat flow q_B at the bottom of the layer can be computed if temperature T and heat flow q at the top of the layer are known:

$$T_B = T + \frac{q_B}{k}\Delta z - \frac{A\Delta z^2}{2k} \quad (4)$$

We obtain crustal geotherms by an iterative method. We discretize depth in layers of 100 m, in order to take into account vertical variation of A and k , and compute T and q at the top and bottom of each layer. The thermo-physical parameters as a function of depth and temperature are modeled following *Chapman* [1986], with the crust subdivided in two layers, upper and lower. Thermal conductivity is a function of temperature and depth:

$$k(T, z) = k_0(1 + cz)/(1 + bT) \quad (5)$$

At zero depth and temperature, k_0 are 3.0 and 2.6 W/m⁻¹K⁻¹, respectively, for the upper and lower layer. Temperature coefficient b for the upper layer is 1.5·10⁻³ K⁻¹ and 1.0·10⁻⁴ K⁻¹ for the lower one. Pressure coefficient c is 1.5·10⁻⁶ m⁻¹ for both layers. In the upper layer, heat production A decreases exponentially with depth, i.e., $A(z) = A_0 \exp(-z/D)$ until the value chosen for the lower crust (0.45 μW m⁻³) is reached. Heat production at surface (A_0) is a function of the surface heat flow $A_0 = 0.4 q_0/D$. We thus assume 40 % of surface heat flow due to shallow radiogenic sources, with depth parameter D set to 8 km. The top of the lower layer is set at 16 km, its bottom at 35 km. We choose to keep these two parameters constant for two reasons: i) we do not aim to obtain a refined thermal model, but a simplified one that we can use as reference; ii) crustal thickness and surface heat flow are uncorrelated, as pointed out by *Mareschal and Jaupart* [2013], implying that radiogenic heat production does not increase with increasing crustal thickness.

This modeling of crustal thermal state presents limitations such as uncertainties in lateral and vertical variations of thermal conductivity and heat production, uncertainties in the heat flux values from the global map, non steady state conditions and lateral heat transfer [*Jaupart and Mareschal*, 2010]. The definition of an accurate crustal thermal model and an investigation of the previously mentioned limitations are outside the scope of the present work. Here we are mostly interested in understanding the general effects of temperature on crustal seismic velocities and density. Our thermal model (Figure 2) is sufficient for this purpose. The thermal model is used for the computation of the forward models and shown as a reference for the comparison of the temperature profiles obtained inverting CR1 V_p data (inverted models).

2.4. Isostatic Topography and Gravitational Field

For calculating isostatic topography, we follow a standard approach [*Lachenbruch and Morgan*, 1990]. We set to zero the mantle lithospheric thickness since we are not interested in lithospheric mantle structure and we want to isolate the crustal effects. We assume a homogeneous value of 3200 kg/m³ for asthenosphere density. Crustal density is computed by a weighted average over depth according to layers thickness for each grid cell of the model.

We further explore the implications of the differences between CR1 and our density models by computing the gravitational field. Forward modeling of the gravitational field is performed using the software *Tesseroids* [*Uieda et al.*, 2011]. Each crustal layer is subdivided in rectangular prisms with a 1 × 1 degree of surface and height equal to the layer thickness. The rectangular prisms are then transformed into spherical

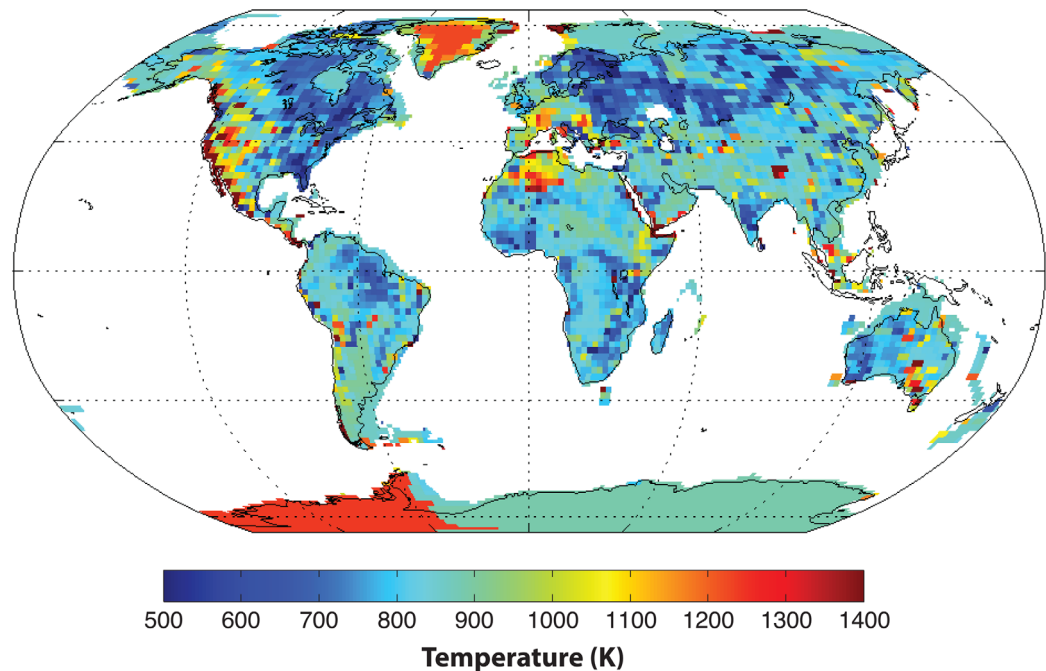


Figure 2. Temperature at 35 km of depth for our thermal model.

prisms, a more suitable geometry when dealing with global gravity modeling as it permits to account for Earth's curvature. The gravitational attraction is then computed as in *Grombein et al.* [2013].

3. Results

3.1. Physical Properties as a Function of P-T and Composition

Variations in P-T affect seismic velocities and density of rocks by modifying the stable mineralogical assemblage and varying the elastic moduli and density of minerals. In order to visualize separately the effects of pressure and temperature, we show V_p as a function of depth (pressure) at given temperatures for the tested compositions (Figure 3, V_s and density are shown in supporting information Figures S1 and S2). H_2O has similar effects on the physical properties obtained with the compositions tested, therefore only hydrated RG (RG025, RG050) are shown. We plot properties at temperatures that correspond to average T for upper, middle and lower crust according to a cold and a hot geotherm (heat flow of 0.040 W/m^2 and 0.080 W/m^2 respectively). We also show how V_p varies for the mineralogies (Table 2) used for computing inverted and forward metastable models (Figure 3, black lines). Showing the physical properties variations for both varying and fixed mineralogies allows a better evaluation of the effects of phase reactions on seismic velocities and density. The increment in depth (pressure) leads to phase transformations. An important reaction is the plagioclase breakdown and the consequent stabilization of clinopyroxene (Figure 3e). The depth of this reaction is controlled by temperature (Figures 3b and 3e), while it is unaffected by variations in major element chemistry. Presence of H_2O , however, does affect the sharpness of the transition. In particular, wet compositions are characterized by a sharper increase in V_p than dry ones. RG and SH compositions produce rocks with significantly different physical properties, especially in the middle and lower crust. In the latter, at a depth of approximately 15 km or higher, RG gives a V_p that is $\sim 4.2\%$ higher than the estimated value for SH at the same temperature (Figure 3c). The presence of H_2O influences mineralogy and consequently has an impact on physical properties. An example of induced mineralogical variations when 0.25 wt. % of H_2O is added to a dry composition is given in Table 2, where stable mineralogies at various P-T conditions are reported for the compositions RG and RG025. The effect of H_2O is not uniform at varying P-T. For instance, at shallow depths of upper and middle crust (Figures 3a and 3b), wet compositions give higher velocities (and density) than the respective dry compositions, but we observe the opposite pattern moving deeper. At low pressure, hydrous compositions give higher seismic velocities because H_2O stabilizes

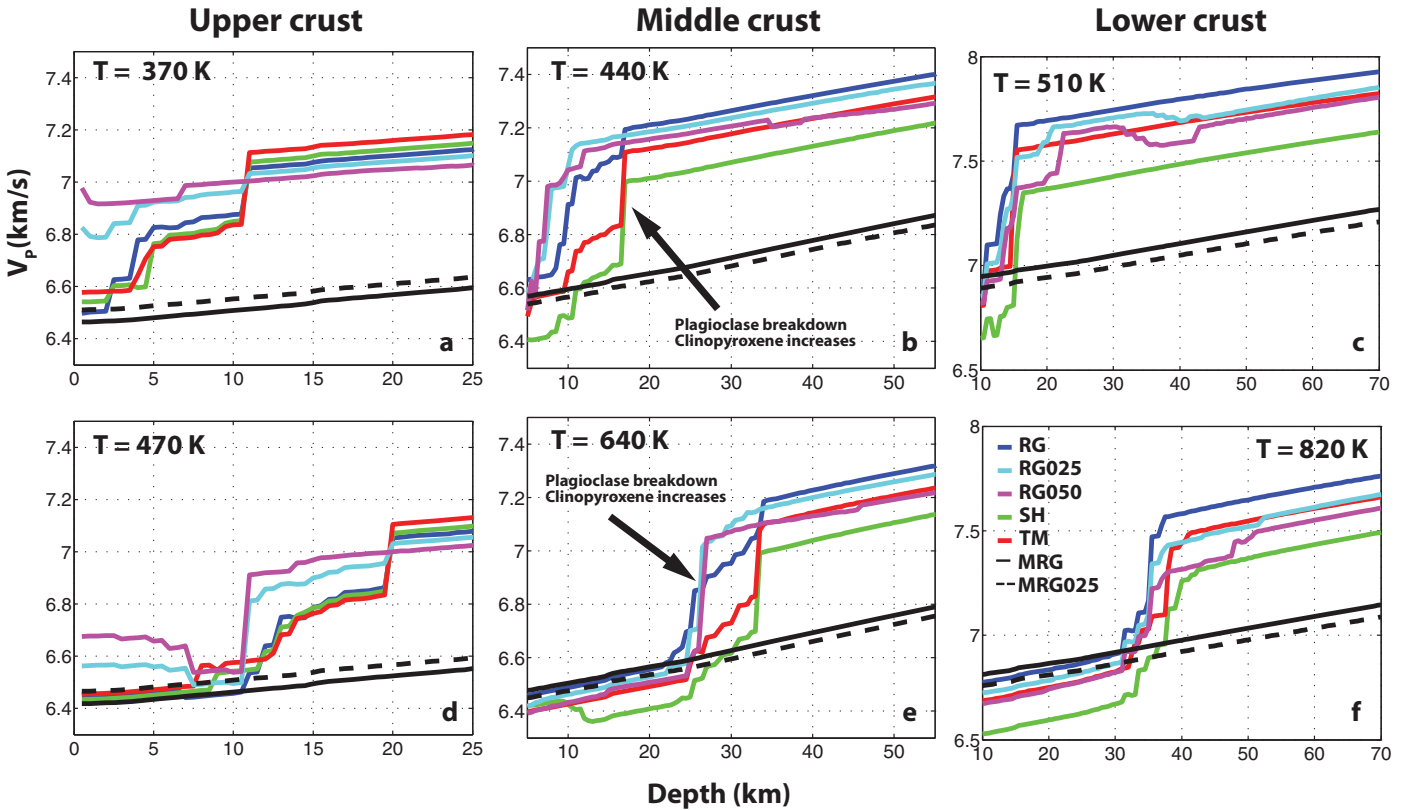


Figure 3. V_p variations with depth at constant temperatures corresponding to (top) cold and (bottom) hot geothermal environments. We consider different chemical compositions at thermodynamic equilibrium and fixed mineralogies. Note the drastic variation of V_p when mineralogical reactions are taken into account and the effect of temperature on the depth of the plagioclase-clinopyroxene reaction. MRG and MRG025 refer to the properties obtained for the fixed mineralogies reported in Table 2.

amphibole at the expense of feldspar. As pressure increases, anhydrous rocks have a higher proportion of clinopyroxene than hydrous rocks. This effect leads to higher wave speeds in the anhydrous rocks. A linear increase with depth of modeled physical properties is observed when metastable mineralogies are considered (Figure 3, black solid and dashed line). In this case, temperature alone has a mild effect. For example, at 20 km depth, the MRG mineral assemblage has a velocity of 6.65 km/s at 440 K (Figure 3b) and 6.57 km/s at 640 K (Figure 3e).

3.2. Analysis of Inverted and Forward Models

We calculate the difference in density, V_p and V_s for each latitude-longitude cell between our models and CR1 (average physical properties for all the models are given in supporting information Tables S2 and S3). The sum of the residuals for each cell, normalized over the total number of cells, gives a global misfit value (M) of the computed models compared to CR1, used as reference:

$$M = \frac{\sum_{i=1}^N \left| \frac{\rho_{mi} - \rho_{CR1}}{\rho_{CR1}} \right|}{N} \cdot 100 \quad (6)$$

where ρ_{mi} is the i -th quantity modeled (in this case density), ρ_{CR1} is the CR1 value, N is the number of latitude-longitude cells for continental areas. A perfect fit gives $M = 0$, while a uniform difference of 50% will give a value of $M = 50$. The same misfit criterion is used to compare the inverted temperatures with our reference thermal model. The misfit is computed both for the vertical average of the entire crust and for each layer singularly. Note that the total crustal misfit is usually lower than the single layer one (see Table 3). This happens because the generally positive residuals in the upper crust are balanced by negative residuals in the lower crust (Figure 4).

The "equilibrium inverted models" (EIRG, EIRG025, EIRG050, EISH, EITM) have a density misfit with CR1 that ranges from 0.44 to 1.1 (Table 3). All the inverted models have lower density than CR1 in the upper and

Table 3. Misfit Between Inverted Models and CR1

	Upper Crust	Middle Crust	Lower Crust	Average Crust
<i>EIRG</i>				
Temperature	153.31	44.84	30.28	61.48
V_S	9.88	2.68	1.76	3.91
Density	1.65	1.03	2.56	0.44
<i>EIRG025</i>				
Temperature	88.19	27.20	18.98	27.54
V_S	4.78	2.73	1.75	2.50
Density	1.21	0.85	3.23	0.68
<i>EIRG050</i>				
Temperature	71.74	23.77	18.69	22.52
V_S	4.02	3.05	2.00	2.65
Density	1.22	0.63	3.68	0.83
<i>EISH</i>				
Temperature	169.04	23.97	15.812	46.70
V_S	9.57	2.85	2.11	2.58
Density	2.46	3.20	2.56	1.10
<i>EITM</i>				
Temperature	186.61	33.83	24.53	60.51
V_S	11.32	1.76	1.42	4.04
Density	2.52	2.43	4.08	0.71
<i>MIRG</i>				
Temperature	183.58	58.85	38.54	75.41
V_S	1.09	0.60	2.08	0.55
Density	2.03	1.41	1.59	0.85
<i>MIRG025</i>				
Temperature	206.50	54.82	33.56	80.03
V_S	2.50	1.36	1.58	1.05
Density	1.50	1.24	2.04	0.66

middle crust, but they are denser in the lower crust (Figure 4). The model EIRG has a similar density structure to CR1 ($M = 0.44$). The match between EIRG and CR1 is particularly good in the middle crust and in regions of *Extended Crust* and *Platform* (Figure 4). The effect of porosity (misfit values for the models corrected for porosity are in supporting information Table S4) is negligible in the lower crust, but becomes more important in the upper crust. However, the porosity effect on density is always of second-order compared to composition. The total misfit in V_S ranges from 2.5% (EIRG025) to $\sim 4\%$ (EITM). The major discrepancies are observed in the upper crust. In general, the misfit decreases from the top layer to the bottom one. For example, EIRG has a misfit of 9.88, 2.68 and 1.76 for upper, middle and lower crust, respectively. In Table 3, we also report the misfit between inverted temperatures and the reference thermal model (section 2.3, parameterized according to CR1). M ranges from 22.52 (EIRG050) to 61.48 (EIRG025).

The misfit decreases from the upper to the lower crust. Accounting for porosity reduces the misfit between inverted temperatures and thermal reference model in the upper crust (Table S4). The effects on middle and lower crust are instead negligible. The "equilibrium forward models" (EFRG, EFSH, EFTM, EFRG025, EFRG050) show a stronger discrepancy with CR1 than the inverted ones, for both density and seismic velocities (Table 4). Models computed considering metastable mineralogy present discrepancies with CR1 that are comparable to those shown by the equilibrium models except in the upper crust, where metastable models present a better fit in V_S .

In general, the misfit between all our models and CR1 is significant and shows a strong variation both horizontally, between different crustal types, and vertically, between upper, middle and lower crust. For example, in the *Archean* lower crust, EIRG025 presents a density distribution in agreement with CR1, but the misfit between the two models is high in the crustal type *Orogen*. The model EIRG, while showing a good match in density for the *mid/late Proterozoic* middle crust, has a high misfit with CR1 in the lower crust for the same crustal type.

4. Discussion

4.1. Thermodynamic Modeling of Crustal Physical Properties

Our methodology deals directly with composition, as an input parameter, enabling us to test proposed crustal chemical models against observations and obtaining insights on their reliability. In addition, our approach is able to model rocks characterized by same seismic velocities but different density or vice versa: an occurrence well known in the literature [e.g., Birch, 1960, 1961; Christensen and Mooney, 1995]. We also consider the nonuniqueness in the relationships between either compressional or shear waves velocity and composition. All these features represent improvements compared to empirical approaches such as those in Christensen and Mooney [1995] and Brocher [2005]. In empirical relations each value of V_p is associated to a single value of V_S and density and there is no direct control on composition. Another difference respect to empirical relationships is that our procedure accounts for coupled effects of pressure and temperature (Figure 3). The variation of P-T conditions inside the crust modifies the identities and amounts of the stable minerals. Variations in the stable mineralogy can be smooth, thus determining a gradual change in density and seismic velocities, or sharp as, for example, the drop in the plagioclase percentage (with a relative increase

The misfit decreases from the upper to the

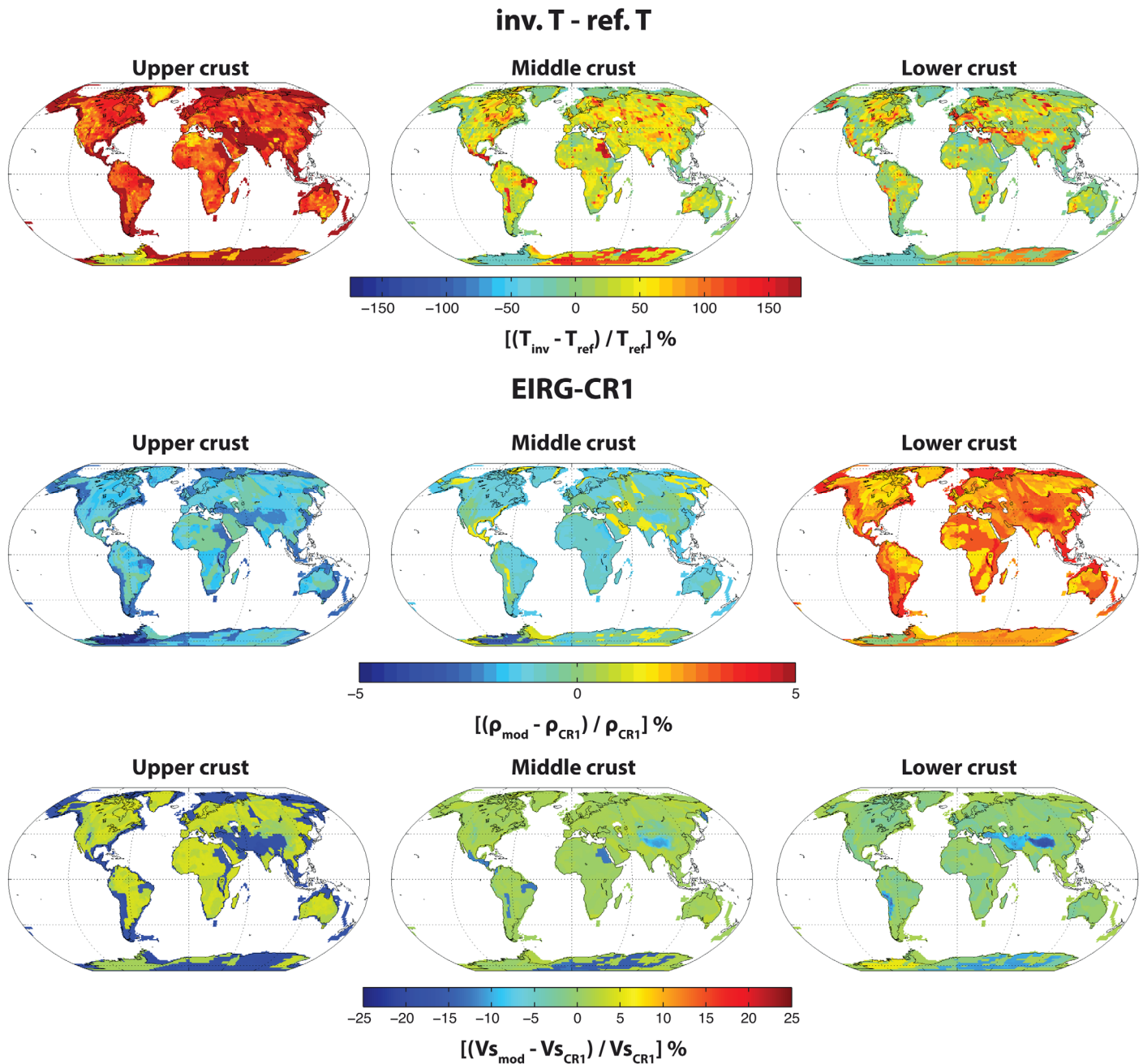


Figure 4. (top) Comparison between inverted temperature (for the model EIRG) and our reference thermal model. (middle and bottom) Comparison between EIRG density and V_s structure with the CR1 values.

in pyroxene amount), leading to an abrupt increase in seismic-wave velocities and density (Figure 3e). Temperature alone does not have a strong effect on physical properties if mineralogy is not allowed to change (Figure 3, solid and dashed line), but it is an important factor if phase transformations are possible, for example, the breakdown of plagioclase (Figures 3b and 3e). The abundance of H₂O is another important factor in determining crustal physical properties. Adding a small amount of H₂O to RG composition leads to similar properties to those obtained by modeling purely dry SH and TM compositions (Figure 5). This result illustrates the sensitivity of rock properties to small amounts of H₂O (in this case 0.25 and 0.50 wt. %). This sensitivity shows that it is difficult to estimate crustal composition solely from seismic velocities. A combined analysis of density and V_p does help to discriminate between rocks characterized by same seismic velocities, but different composition (Figure 5).

Table 4. Misfit Between Forward Models and CR1

	Upper Crust	Middle Crust	Lower Crust	Average Crust
<i>EFRG</i>				
V_p	9.74	4.66	5.19	5.91
V_s	11.97	5.83	6.29	7.09
Density	4.92	3.35	6.60	4.67
<i>EFRG025</i>				
V_p	11.20	5.01	5.41	6.21
V_s	14.59	6.92	7.79	8.49
Density	6.28	3.70	6.12	5.06
<i>EFRG050</i>				
V_p	11.80	4.68	5.02	5.97
V_s	15.96	7.04	7.35	8.79
Density	6.69	3.43	5.54	4.91
<i>EFSH</i>				
V_p	9.43	2.71	4.23	3.54
V_s	10.98	3.81	5.33	4.98
Density	3.55	3.49	4.31	2.55
<i>EFTM</i>				
V_p	9.53	3.26	4.50	4.56
V_s	10.25	3.87	5.60	5.17
Density	3.35	2.40	5.97	3.14
<i>MFRG</i>				
V_p	6.44	2.80	2.22	3.06
V_s	7.52	3.27	2.36	3.19
Density	1.22	1.46	2.16	1.27
<i>MFRG025</i>				
V_p	7.19	2.57	2.20	2.90
V_s	9.14	3.62	2.37	3.80
Density	1.82	1.45	2.14	1.39

Our results indicate that discontinuous changes in physical properties within the crust can be due to variations in stable mineralogy rather than to stratification of chemical composition. The main mineralogical transitions occur at a similar depth range for all the tested compositions (Figure 3). Phase reactions, therefore, can play an important role even in case of a large degree of chemical heterogeneity within the crust.

The differences between physical properties obtained with various chemical models are significant, particularly in the middle and lower crust, i.e., where fewer direct constraints on composition are available. The proposed chemical models for the deeper parts of the crust mostly rely on analysis of (i) high-grade metamorphic terrains, (ii) deep crustal xenoliths, and (iii) seismic velocity constraints. The first two

sources, though direct, offer a limited amount of information, especially on the spatial scale. Interpretation of seismic velocities in terms of petrology and chemical composition is not straightforward. So far, such interpretation has been carried out on the basis of empirical relationships, with the limitations discussed earlier. Our study shows how the interpretation is affected when phase transformations and material properties are taken into account. For example, we find that mid crustal rocks can have seismic velocities typical of the lower crust ($V_p > 7.0$ km/s), suggesting that a mafic composition is not needed to explain lower crust seismic wave speeds, as already proposed elsewhere [Hacker *et al.*, 2011, 2015].

4.2. Continental Crust Models

We have investigated the way relationships based on thermodynamical modeling affect inferred physical properties (Tables 3 and 4). The comparison between inverted models and CR1 is particularly useful since these models are based on the same V_p structure, but V_s and density are inferred using different approaches. The discrepancies are strong. For example, the misfit in density, which ranges between 0.44

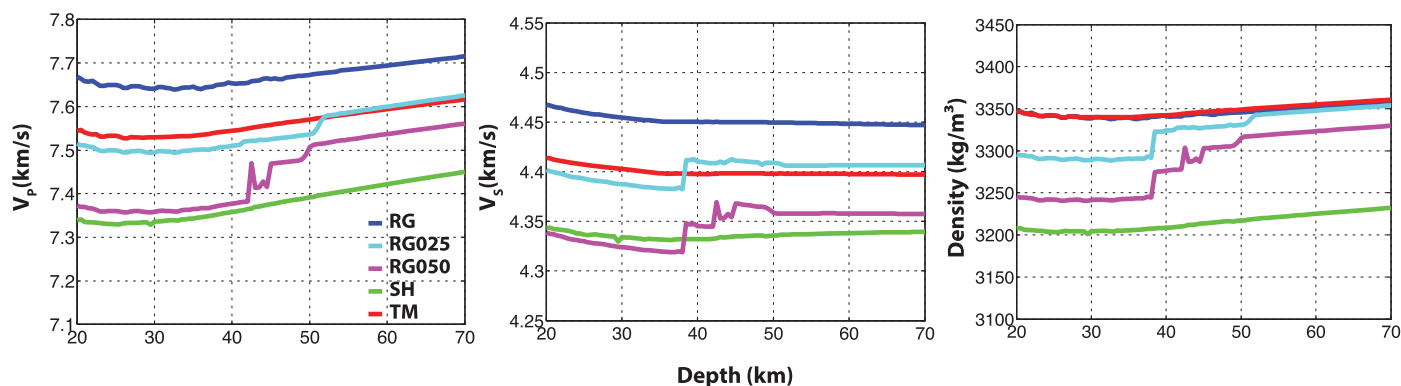


Figure 5. Variation with depth of physical properties computed for lower crust compositions along a continental geotherm with a surface heat flow of 0.045 W/m^2 . RG025 and RG050 show approximately the same seismic velocities of TM and SH, respectively.

and 1.1, translates into remarkable effects on isostatic topography and gravity (see section 4.5). The density of our models has a particularly high misfit with CR1 in the lower crust (Table 3). This can be due to the fact that the empirical relationships used in CR1 [Brocher, 2005] are not able to properly account for coupled P-T effects on physical properties.

The misfits in Tables 3 and 4 are evidently affected by uncertainties in the computed physical properties. Regarding this point CR1 properties are surely uncertain, but the uncertainties are not quantified. The physical properties obtained with the thermodynamic modeling are affected by errors that are not constant, depending on the P-T conditions at which the properties are evaluated, the phases involved in the calculation, their percentage and chemical composition, and the uncertainties on the thermodynamic parameters of the specific end-members. For a single crystal, at a given P-T condition, the errors on seismic velocities are <2%, and even less for densities [Hacker *et al.*, 2003]. Considering that the misfit are relative to values averaged on the thickness of a single layer or of the entire crust, it is not trivial to assess the effects of physical properties uncertainties on the computed models. Since we have tested various compositional models, resulting in significantly different physical properties, and since none of our models matches CR1, we maintain that our general results are robust. The difficulty in reconciling proposed continental crust physical properties with available estimates of chemical composition poses a caveat on our present understanding of the continental crust thermal and compositional state. In spite of current uncertainties, the methodology presented in this work is suitable to obtain a new generation of crustal physical properties models with a coherent meaning in terms of thermo-chemical structure.

4.3. Inverted Temperatures

The temperature structures obtained for the inverted models are governed by various factors: i) input composition, ii) thermodynamic constraints, iii) CR1 layers thicknesses (that constrain pressure) and iii) CR1 V_p model. These factors present uncertainties that lead to discrepancies between inverted and reference temperatures (obtained as explained in section 2.3). Chemical heterogeneity in the continental crust, which was not considered here, may also contribute to these discrepancies. Likewise, metastability can have a strong influence on inverted temperatures. In regions where seismic waves sample metastable lithologies, the inverted temperatures are more representative of the conditions at which the metastable rocks last equilibrated, than they are of present-day temperature.

The misfit with the reference temperatures decreases from the upper to the lower crust (Table 3) independently of the composition used. This result can be attributed to various sources: i) a higher quantity of metastable rocks in the upper crust compared to middle and lower crust, ii) an upper crust relatively richer in hydrated phases, iii) influence of porosity and fractures on seismic velocities. The first hypothesis is based on the fact that equilibration mechanisms are essentially thermally activated and middle and lower crust are at a higher temperature than the upper crust. Our test with fixed reference mineralogies (Table 2), however, is not able to bring temperatures closer to expected ones in the upper crust. Note that these mineralogies are computed by considering average P-T values for upper, middle and lower crust: an approach that is not fully able to model the extremely heterogeneous petrology of the upper crust. The second hypothesis comes from the strong effect of H₂O on physical properties. Adding even a low amount of it, 0.25 wt. % for example, helps reducing the misfit in the upper crust. A similar, but weaker effect is also observed in middle and lower crust (Table 3). The third hypothesis relates to the seismic waves velocity decrease in presence of pores and fractures. The effect is mostly confined to the upper crust. Including porosity in our modeling reduces the differences between inverted and reference temperatures, particularly in the upper crust, the misfit however remains still high (see supporting information Table S4).

We further analyze the discrepancy between inverted temperatures and reference geotherms in different CR1 crustal types (Figure 6). The offset between them is always very high in the upper crust, but significantly decreases in middle and lower crust, reaching a minimum after the average bottom of the middle crust. Large differences are again observed in the deepest regions, especially in the crustal type *Orogen* where the crust is particularly thick. We observe an increase in the offset between reference and inverted temperatures also in the lower crust of the *Extended Crust*. Considered chemical compositions cover the expected range of variations in major elements. For example, SiO₂ varies from 65.9 in TM to 66.8 in SH. If we assume that the CR1 V_p values are reliable, our results suggest that the upper crust is mostly characterized by

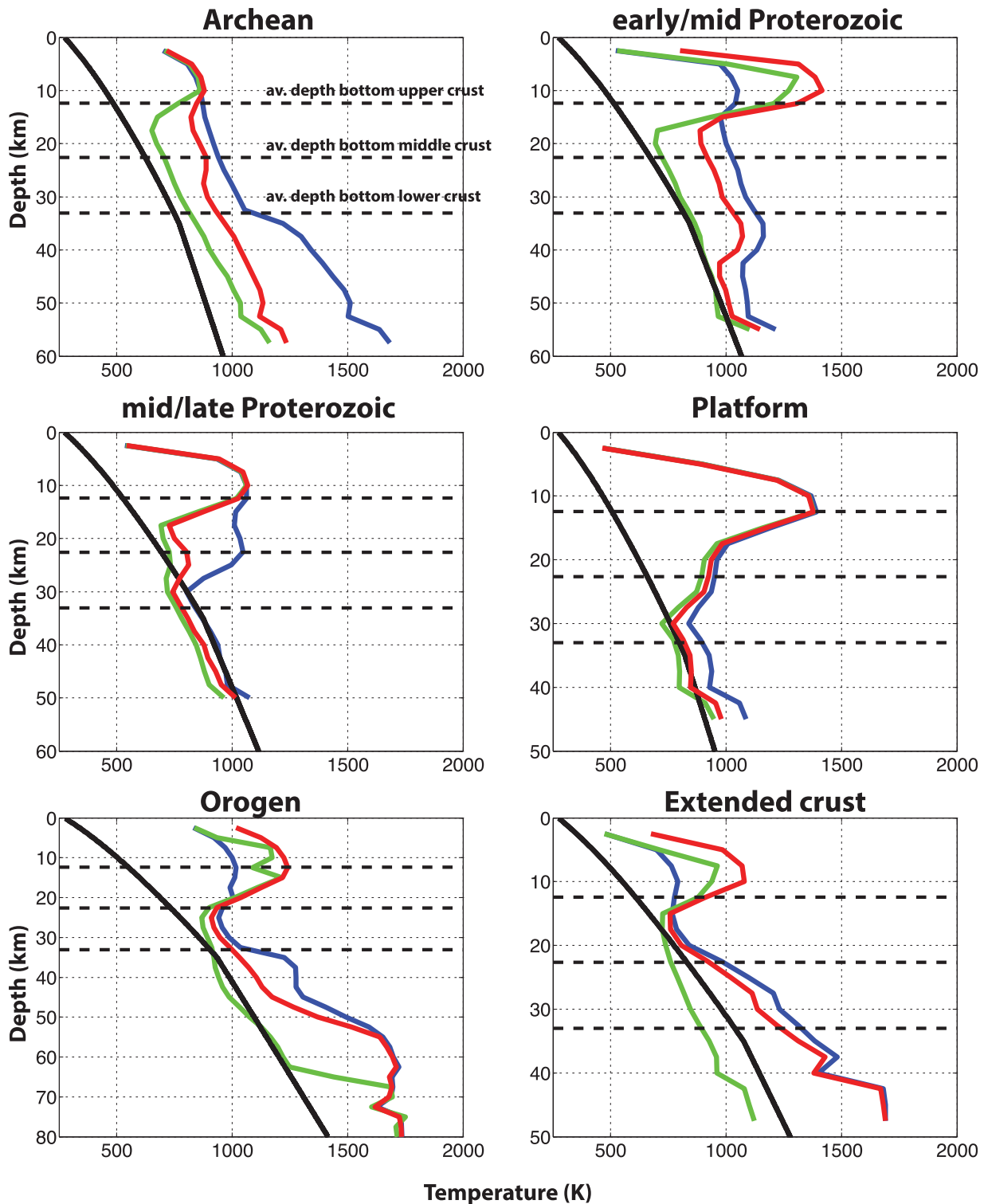


Figure 6. Inverted temperature obtained for various crustal types. Temperature at each depth is computed as the horizontal average considering only the specified crustal type. Blue line = model EIRG, green line = model EISH, red line = model EITM. Black line is for the reference thermal model (computed as described in section 2.3). Black dashed lines represent average depth of the bottom of the upper, middle, and lower crust for the specified crustal type.

metastable mineralogies, while higher temperatures in the middle and lower crust have favored processes of thermodynamic equilibration. In the *Orogen* crustal type, where crustal thickness exceeds 60 km in some areas (Andes, Himalaya), metastable mineralogies can again become dominant in the lower crust. This result

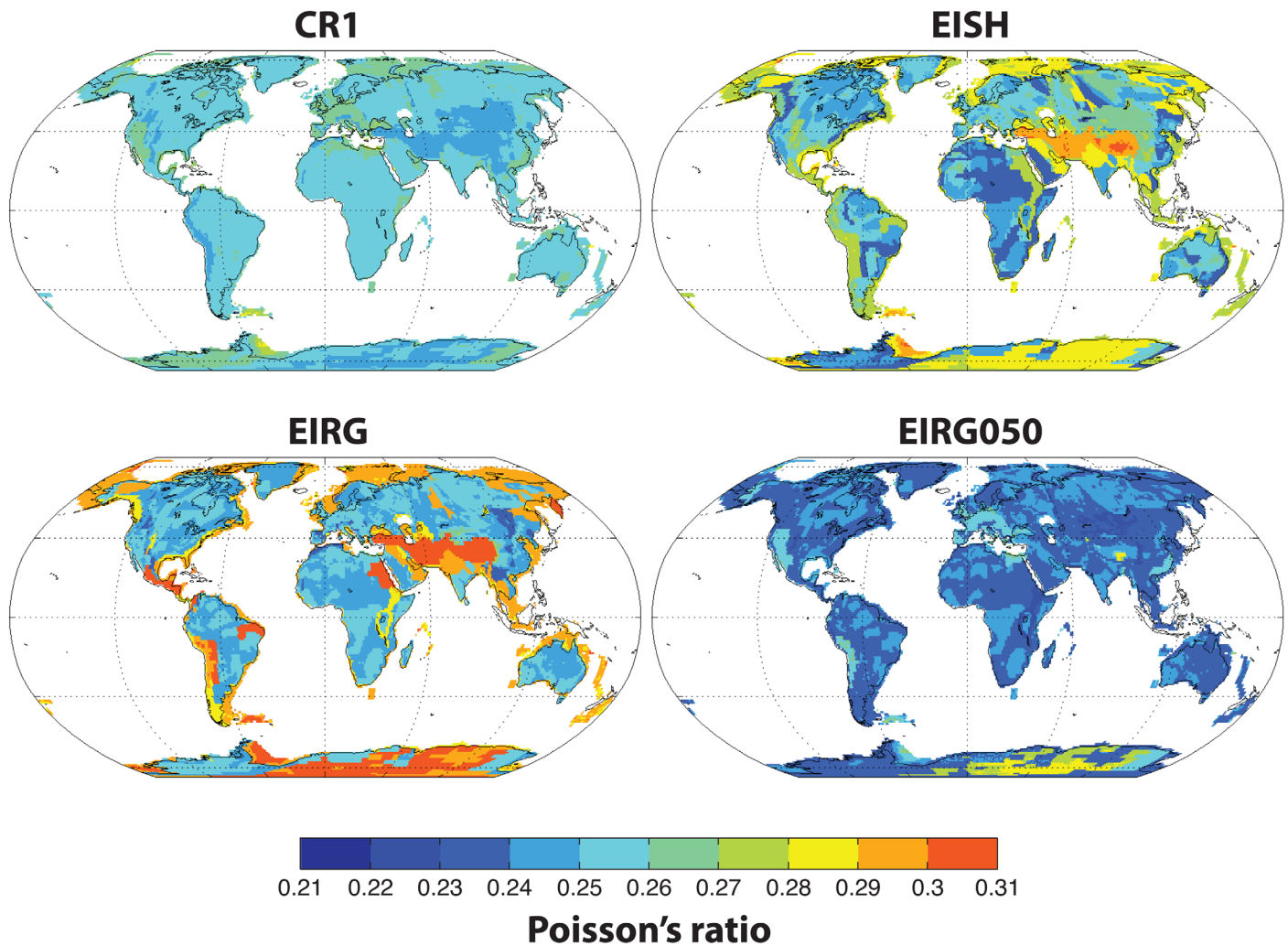


Figure 7. Poisson's ratio computed for CR1 and some inverted models. Models obtained with dry compositions (EIRG, EISH) are in general agreement with CR1 with the exception of the crustal type *Orogen*.

is in agreement and supports previous findings that require metastable rocks at the roots of mountain belts to maintain mechanical stability [Jackson *et al.*, 2004]. In the *Extended Crust* instead, the increase of the offset between inverted and reference thermal profiles observed in the lower crust can be associated with underplating of mafic magmas [Zandt and Ammon, 1995] and the consequent variation in chemical composition. However, the assumed steady state approximation for the reference thermal model is not fully appropriate in both *Orogen* and *Extended Crust* crustal types where recent and/or ongoing thermo-mechanical processes influence the thermal state. Consequently, the reference geotherms in these areas are not particularly robust.

4.4. Poisson's Ratio and Crustal Composition

The relation between V_p and the rocks mineralogy is nonunique. The analysis of the Poisson's ratio, i.e., $\sigma = 1/2\{1 - [(V_p/V_s)^2 - 1]^{-1}\}$, rather than V_p alone, does permit qualitative discrimination between rock types [Christensen, 1996; Zandt and Ammon, 1995]. For crustal rocks it is possible to interpret σ in terms of silica content, being the two parameters anticorrelated. This is mostly due to the anomalous low value of quartz σ (~ 0.056) [Levien *et al.*, 1980].

The average Poisson's ratio in Archean crust for CR1 is ~ 0.25 . The value is significantly lower than Zandt and Ammon [1995] value for Precambrian shields ($\sigma = 0.29 \pm 0.02$). Chevrot and van der Hilst [2000], in a study focusing on Australian crust, also obtained a high σ (~ 0.28) in most of the stations located in Archean

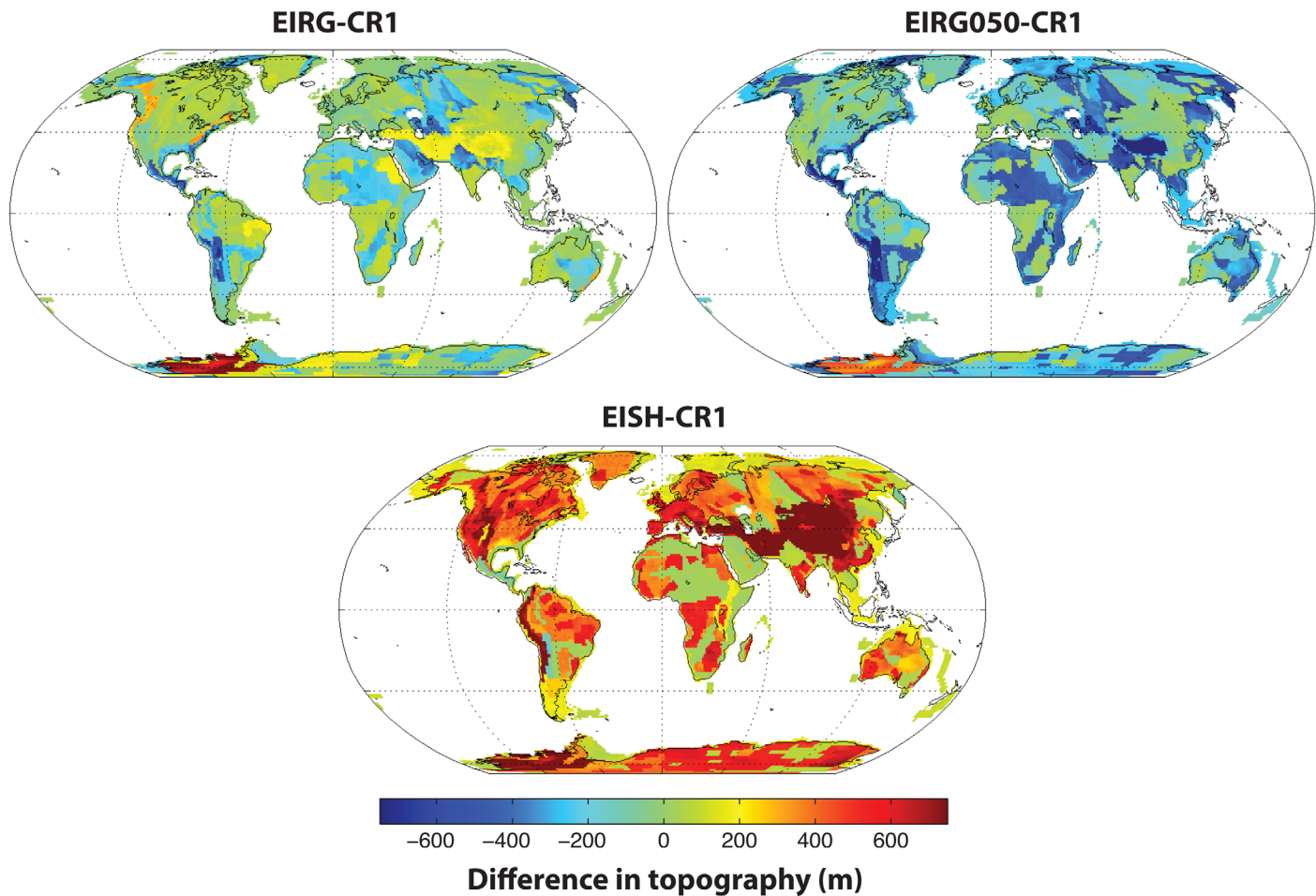


Figure 8. Difference in isostatic topography computed considering CR1 and some of the inverted models.

terrains. Assuming a felsic to intermediate composition for upper and middle crust, as suggested by various observations [Rudnick and Gao, 2003], high values of σ imply the presence of a mafic lower crust, which is related to a process of underplating and/or intrusion of mafic melts at the base of the crust [Zandt and Ammon, 1995]. Other studies, however, estimated Poisson's ratio in Archean crust that are closer to the obtained σ from CR1. Youssef *et al.* [2013] found $\sigma \sim 0.26$ in South African cratonic regions. Egorkin [1998] obtained $\sigma \sim 0.25$ in the Siberian Precambrian cratons.

For the lower crust, CR1 presents an average σ of 0.26 in both Archean and Proterozoic crustal types. If real, such low values of σ would have important implications on crustal formation and evolution. One of the possible processes leading to crust formation is the tectonic amalgamation of island arcs and oceanic plateaus [Rudnick and Fountain, 1995]. In this case, a considerable amount of mafic material would be added to the crust, determining a high σ . If Archean and Proterozoic crust are characterized by low σ , it implies that the mafic portion has been somehow removed, probably thanks to a delamination process [Bird, 1979]. Alternatively, it could be that the crust-forming Precambrian processes were sensibly different from the current mechanisms for crust formation and accretion [Rudnick, 1995].

Similarly to CR1, inverted models show intermediate σ in the lower crust of cratonic areas. The highest values occur in Archean (0.28) and early/mid Proterozoic crust (0.28) in EIRG. EIRG has a lower crust composition with 53.4 wt.% SiO₂. The addition of just 0.50 wt.% of water reduces σ to 0.26 for the Archean crust and to 0.27 for the early Phanerozoic crust. The obtained values are comparable to those estimated for SH composition, which has 58.3 wt. % SiO₂ in the lower crust. This result shows, once again, the effectiveness of a small quantity of water in changing rocks physical properties. Thus, without

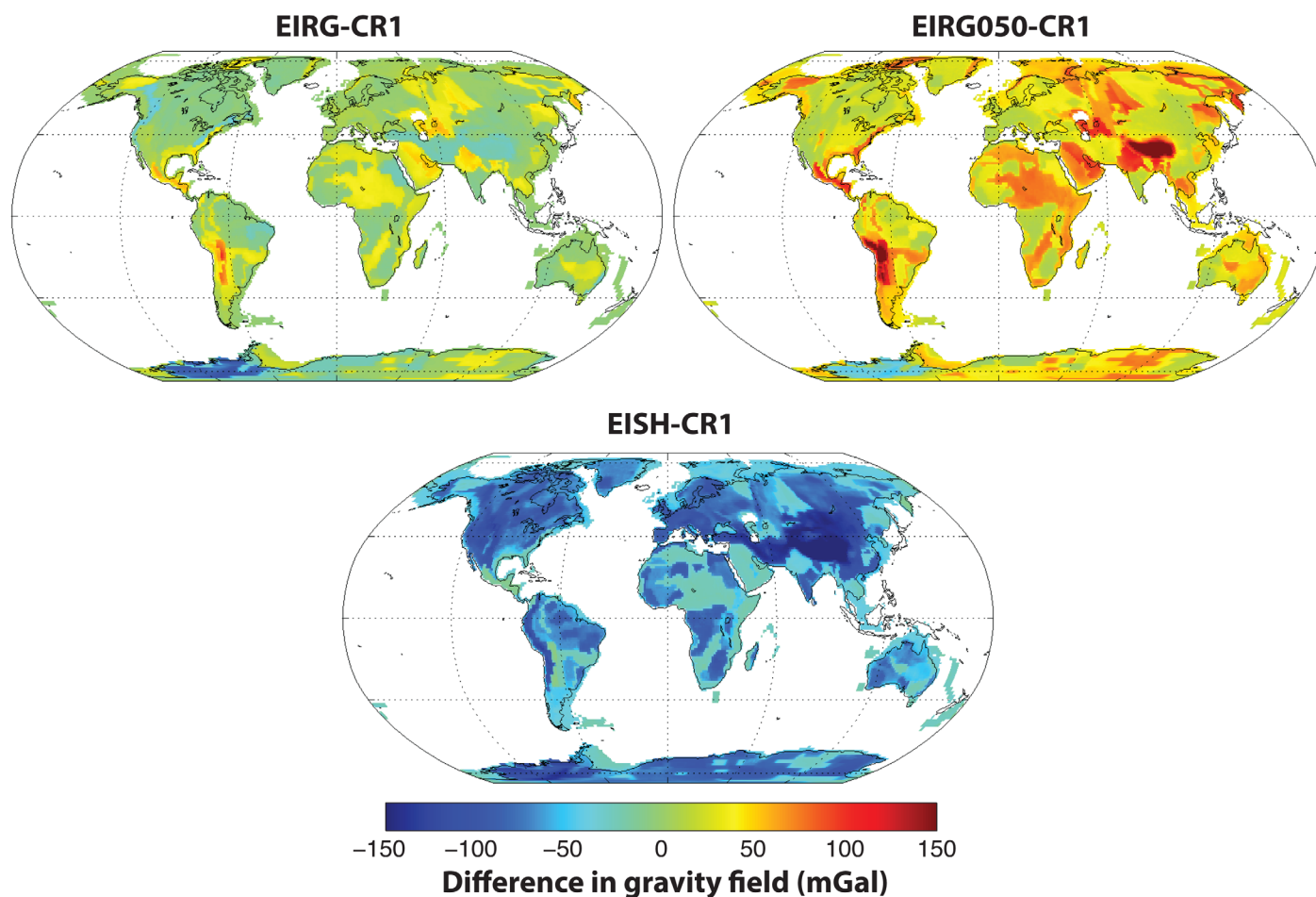


Figure 9. Differences in the gravity fields computed with CR1 density models and with some of our inverted density models.

independent knowledge of H₂O-content, crustal composition is poorly constrained even by V_p/V_s and Poisson's ratio.

The Poisson ratios of the crustal type *Orogen* are very different between CR1 and our models. In CR1, the lower crust of *Orogen* has the lowest σ , especially in regions with thick crust (below the Andes and Himalaya). In our inverted models, instead, we observe the highest σ in these regions (Figure 7). The discrepancy is probably due to coupled P-T effects on stable mineralogy that are accounted for in our methodology, while being neglected in CR1.

4.5. Density Differences and Effects on Topography and Gravity

The difference in average density distribution between inverted models and CR1 ranges approximately from -100 to $+100$ kg/m³. To better understand the implications of these differences, we compute isostatic topography for various models. In general, variations between synthetic topography computed with CR1 and our inverted models exceed ± 600 m (Figure 8). It is straightforward to understand the importance of such large differences. Studies of dynamic topography are an example. Dynamic topography is characterized by a maximum amplitude of ~ 1000 m [Braun, 2010]. A proper modeling of crustal density and its static effect on topography is therefore fundamental to obtain reliable estimates of residual topography, to which compare models of dynamic topography.

We also analyze the effects on gravitational field. Differences between models range from ± 150 mGal (Figure 9). Also variations in gravity are remarkably large and they evidence the utility of gravity data to better constrain the density structure of the crust, and, consequently, its chemical composition.

Table 5. Average V_p/V_s , V_p/ρ and V_s/ρ for EIRG and CR1

	Upper Crust	Middle Crust	Lower Crust
Archean	EIRG – CR1		
V_p/V_s	1.69–1.72	1.72–1.73	1.80–1.75
V_p/ρ	2.29–2.25	2.30–2.28	2.30–2.34
V_s/ρ	1.36–1.30	1.34–1.32	1.28–1.34
Early/mid Proterozoic			
V_p/V_s	1.80–1.73	1.81–1.75	1.80–1.75
V_p/ρ	2.25–2.22	2.30–2.28	2.30–2.35
V_s/ρ	1.26–1.28	1.28–1.30	1.28–1.34
Mid/late Proterozoic			
V_p/V_s	1.81–1.74	1.81–1.74	1.77–1.75
V_p/ρ	2.28–2.26	2.31–2.28	2.30–2.37
V_s/ρ	1.27–1.29	1.28–1.31	1.30–1.35
Platform			
V_p/V_s	2.07–1.72	1.70–1.74	1.79–1.76
V_p/ρ	2.26–2.25	2.27–2.31	2.36–2.37
V_s/ρ	1.09–1.30	1.33–1.33	1.29–1.35
Orogen			
V_p/V_s	1.81–1.72	1.74–1.73	1.81–1.74
V_p/ρ	2.28–2.23	2.29–2.28	2.28–2.35
V_s/ρ	1.27–1.30	1.32–1.32	1.26–1.35
Extended			
V_p/V_s	1.68–1.72	1.71–1.73	1.81–1.83
V_p/ρ	2.29–2.23	2.30–2.27	2.28–2.31
V_s/ρ	1.37–1.30	1.34–1.31	1.26–1.26

4.6. Ratio of Physical Properties

The average ratios between physical properties computed for the model EIRG are given in Table 5 (also ratios from CR1 are listed for comparison). We present the ratios for six continental crustal types (*Archean, early/mid Proterozoic, mid/late Proterozoic, Platform, Orogen and Extended crust*), that together account for approximately 70 % of the entire continental crust (areal coverage) according to CR1. Our ratios are significantly different than those from CR1 and can be used as an alternative to relate the physical properties considered.

In the main text, only ratios for EIRG model are given. Values for all other models are available at <http://ign.ku.dk/english/employees/geology/?pure-en/persons/427925>. The EIRG ratios are based on CR1 V_p data and on the

Rudnick and Gao [2003] chemical composition, which has a SiO₂ content in between the other two considered compositions.

4.7. Future Directions

Understanding the thermo-chemical state of the crust remains a challenging task because of limited resolution of geophysical models, their nonuniqueness and strong chemical and thermal heterogeneity within the crust. To cope with these issues, the best approach is to interpret multiple geophysical observations taking into account phase equilibria constraints. Such a methodology has already been proposed to unravel the thermo-chemical structure of the lithosphere and upper mantle [Afonso *et al.*, 2013a; Afonso *et al.*, 2013b]. Future experiments on main crust-forming minerals, particularly targeting the shear moduli and their temperature dependence, are also required to reduce uncertainties and improve further the potential of such a multidisciplinary approach. The application of our methodology may lead to a new generation of crustal physical models with a clear meaning in terms of temperature and composition.

5. Summary and Conclusion

We compute elastic properties of crustal rocks both at thermodynamic equilibrium and for metastable mineralogies (i.e., mineralogies that do not vary with P-T conditions) for proposed chemical compositions of the continental crust. We obtain consistent relationships between seismic velocities and density that take into account P-T effects on elasticity of minerals and phase reactions.

We find that average chemical compositions proposed for the continental crust results in significantly different physical properties. Phase transformations have an important effect on seismic velocities and density. Seismic discontinuities within the crust can be correlated to major metamorphic reactions, and not only to chemical stratification. The addition of even a small amount of H₂O to dry compositions modifies the mineralogical assemblage, producing significant effects on rocks physical properties. Effects due to 0.25 wt. % of H₂O are comparable to those due to variations in major elements between tested compositions.

We analyzed the Poisson's ratio derived from CR1 and our models V_p - V_s structures. Cratonic areas are consistently characterized (in CR1 and our models) by low σ , suggesting a felsic to intermediate composition. The largest discrepancy in σ between CR1 and our models is observed in regions characterized by thick crust, at the roots of mountain belts. Coupled pressure and temperature effects, which are neglected by the V_p - V_s empirical relations adopted in CR1, are probably at the origin of this difference. Since it is possible to

obtain the same Poisson's ratio starting from different compositions and slightly varying the amount of H₂O, we argue that even this parameter has a limited resolving power regarding crustal composition.

The obtained density distributions based on thermodynamically constrained relationships are remarkably different from CR1 density and generate variations in isostatic topography on the order of ± 600 m and in gravitational field of approximately ± 150 mGal.

In view of the nonlinear relationships between seismic velocity, density and composition, we find that it is impossible to univocally infer crustal chemical composition relying on seismic velocities alone. A joint inversion of multiple geophysical observables, combined with mineral physics and phase equilibria constraints, is required.

Acknowledgments

CRUST 1.0 can be downloaded at <http://igppweb.ucsd.edu/~gabi/rem.html>. Perple_x is available at <http://www.perplex.ethz.ch>. Heat flow data used to compute the reference thermal model are available as supporting information of Davies [2013]. Our models are free to download at <http://ign.ku.dk/english/employees/geology/?pure=en/persons/427925>. We thank C.H. Jones, A.R. Lowry, J.C. Afonso and the editor, T.W. Becker for insightful comments that improved the manuscript. We also thank S. Speziale for additional helpful comments. This work is supported by Danish Research Council, Sapere Aude grant 11–105974.

References

- Afonso, J. C., J. Fulla, Y. Yang, J. A. D. Connolly, and A. G. Jones (2013a), 3-D multi-observable probabilistic inversion for the compositional and thermal structure of the lithosphere and upper mantle. II: General methodology and resolution analysis, *J. Geophys. Res. Solid Earth*, *118*, 1650–1676, doi:10.1002/jgrb.50123.
- Afonso, J. C., J. Fulla, W. L. Griffin, Y. Yang, A. G. Jones, J. A. D. Connolly, and S. Y. O'Reilly (2013b), 3-D multi-observable probabilistic inversion for the compositional and thermal structure of the lithosphere and upper mantle. I: A priori petrological information and geophysical observables, *J. Geophys. Res. Solid Earth*, *118*, 2586–2617, doi:10.1002/jgrb.50124.
- Baranov, A. A. (2010), A new crustal model for Central and Southern Asia, *Izv. Phys. Solid Earth*, *46*(1), 34–46.
- Bina, C. R., and G. R. Helffrich (1992), Calculation of elastic properties from thermodynamic equation of state principles, *Annu. Rev. Earth Planet. Sci.*, *20*, 527–552.
- Birch, F. (1960), The velocity of compressional waves in rocks to 10 Kilobar, Part 1, *J. Geophys. Res.*, *65*(4), 1083–1102.
- Birch, F. (1961), The velocity of compressional waves in rocks to 10 Kilobars, Part 2, *J. Geophys. Res.*, *66*(7), 2199–2224.
- Bird, P. (1979), Continental delamination and the Colorado Plateau, *J. Geophys. Res.*, *84*(B13), 7561–7571.
- Braun, J. (2010), the many surface expressions of mantle dynamics, *Nat. Geosci.*, *3*, 825–834.
- Brocher, T. M. (2005), Empirical relations between elastic wavespeeds and density in the earth's crust, *Bull. Seismol. Soc. Am.*, *95*(6), 2081–2092.
- Cammarano, F. (2013), A short note on the pressure-depth conversion for geophysical interpretation, *Geophys. Res. Lett.*, *40*, 4834–4838, doi:10.1002/grl.50887.
- Cammarano, F., S. Goes, P. Vacher, and D. Giardini (2003), Inferring upper-mantle temperatures from seismic velocities, *Phys. Earth Planet. Inter.*, *138*, 197–222.
- Chapman, D. S. (1986), Thermal gradients in the continental crust, *Geol. Soc. Spec. Publ.*, *24*, 63–70.
- Chevrot, S., and R. van der Hilst (2000), The Poisson ratio of the Australian crust: Geological and geophysical implications, *Earth Planet. Sci. Lett.*, *183*, 121–132.
- Christensen, N. I. (1996), Poisson's ratio and crustal seismology, *J. Geophys. Res.*, *101*(B2), 3139–3156.
- Christensen, N. I., and W. D. Mooney (1995), Seismic velocity structure and composition of the continental crust: A global view, *J. Geophys. Res.*, *100*(B7), 9761–9788.
- Clarke, F. W. (1889), *The Relative Abundance of the Chemical Elements*, vol. XI, pp. 131–142, Phil. Soc. Washington Bull., Washington, D. C.
- Connolly, J. A. D. (2009), The geodynamic equation of state: What and how, *Geochem. Geophys. Geosyst.*, *10*, Q10014, doi:10.1029/2009GC002540.
- Davies, J. H. (2013), Global map of solid Earth surface heat flow, *Geochem. Geophys. Geosyst.*, *14*, 4608–4622, doi:10.1002/ggge.20271.
- Dong, H., W. Wei, G. Ye, S. Jin, A. G. Jones, J. Jing, L. Zhang, C. Xie, F. Zhang, and H. Wang (2014), Three-dimensional electrical structure of the crust and upper mantle in Ordos Block and adjacent area: Evidence of regional lithospheric modification, *Geochem. Geophys. Geosyst.*, *15*, 2414–2425, doi:10.1002/2014GC005270.
- Egor'kin, A. V. (1998), Velocity structure, composition and discrimination of crustal provinces in the former Soviet Union, *Tectonophysics*, *298*, 395–404.
- Goldschmidt, V. M. (1933), Grundlagen der quantitativen Geochemie, *Fortschr. Mineral. Kinst. Petrogr.*, *17*, 112.
- Grombein, T., K. Seitz, and B. Heck (2013), Optimized formulas for the gravitational field of a tesseroid, *J. Geod.*, *87*, 645–660.
- Hacker, B. R., and G. A. Abers (2004), Subduction factory 3: An excel worksheet and macro for calculating the densities, seismic wave speeds, and H₂O contents of minerals and rocks at pressure and temperature, *Geochem. Geophys. Geosyst.*, *5*, Q01005, doi:10.1029/2003GC000614.
- Hacker, B. R., G. A. Abers, and S. M. Peacock (2003), Subduction factory 1. Theoretical mineralogy, densities, seismic wave speeds, and H₂O contents, *J. Geophys. Res.*, *108*(B1), 2029, doi:10.1029/2001JB001127.
- Hacker, B. R., P. B. Kelemen, and M. D. Behn (2011), Differentiation of the continental crust by reamination, *Earth Planet. Sci. Lett.*, *307*, 501–516.
- Hacker, B. R., P. B. Kelemen, and M. D. Behn (2015), Continental Lower Crust, *Annu. Rev. Earth Planet. Sci.*, *43*, 6.1–6.39.
- Holland, T. J. B., and R. Powell (1998), An internally consistent thermodynamic data set for phases of petrological interest, *J. Metamorph. Geol.*, *16*, 309–343.
- Jackson, J. A., H. Austrheim, D. McKenzie, and K. Priestley (2004), Metastability, mechanical strength, and the support of mountain belts, *Geology*, *32*, 625–628.
- Jagoutz, O., and M. D. Behn (2013), Foundering of lower island-arc crust as an explanation for the origin of the continental Moho, *Nature*, *504*, 131–134.
- Jaupart, C., and J.-C. Mareschal (2010), *Heat Generation and Transport in the Earth*, Cambridge Univ. Press, Cambridge, Mass.
- Karato, S.-i. (1993), Importance of anelasticity in the interpretation of seismic tomography, *Geophys. Res. Lett.*, *20*(15), 1623–1626.
- Kern, H. (1990), Laboratory seismic measurements: An aid in the interpretation of seismic field data, *Terra Nova*, *2*, 617–628.
- Lachenbruch, A. H., and M. Morgan (1990), Continental extension, magmatism and elevation; formal relations and rules of thumb, *Tectonophysics*, *174*, 39–62.

- Laske, G., G. Masters, Z. Ma, and M. Pasyanos (2013), Update on CRUST1.0: a 1-degree global model of Earth's crust, *Geophys. Res. Abstr.*, *15*, EGU2013-658.
- Levien, L., C. T. Prewitt, and D. J. Weidner (1980), Structure and elastic properties of quartz at pressure, *Am. Mineral.*, *65*, 920-930.
- Ludwig, W. J., J. E. Nafe, and C. L. Drake (1970), Seismic refraction, in *The sea*, edited by A. E. Maxwell, pp. 53-84, Wiley-Interscience, N. Y.
- Mareschal, J.-C., and C. Jaupart (2013), Radiogenic heat production, thermal regime and evolution of continental crust, *Tectonophysics*, *609*, 524-534.
- Meier, U., A. Curtis, and J. Trampert (2007), Fully nonlinear inversion of fundamental mode surface waves for a global crustal model, *J. Geophys. Res.*, *34*, L16304, doi:10.1029/2007GL030989.
- Molinari, I., and A. Morelli (2011), EPCrust: A reference crustal model for the European Plate, *Geophys. J. Int.*, *185*, 352-364.
- Nataf, H.-C., and Y. Ricard (1996), 3SMAC: An a priori tomographic model of the upper mantle based on geophysical modeling, *Phys. Earth Planet. Inter.*, *95*, 101-122.
- Reguzzoni, M., and D. Sampietro (2015), GEMMA: An Earth crustal model based on GOCE satellite data, *Int. J. Appl. Earth Obs.*, *35*, 31-43.
- Ritsema, J., H. J. v. Heijst, J. H. Woodhouse, and A. Deuss (2009), Long-period body wave traveltimes through the crust: Implication for crustal corrections and seismic tomography, *Geophys. J. Int.*, *179*, 1255-1261.
- Rudnick, R. L. (1995), Making continental crust, *Nature*, *378*, 571-578.
- Rudnick, R. L., and D. M. Fountain (1995), Nature and composition of the continental crust: A lower crustal perspective, *Rev. Geophys.*, *33*(3), 267-309.
- Rudnick, R. L., and S. Gao (2003), The composition of the continental crust, in *The Crust*, edited by R. L. Rudnick, pp. 1-64, Elsevier-Pergamon, Oxford, U. K.
- Sato, H., M. C. Fehler, and T. Maeda (2012), *Seismic Wave Propagation and Scattering in the Heterogeneous Earth*, Springer, N. Y.
- Shapiro, N. M., and M. H. Ritzwoller (2002), Monte-Carlo inversion for a global shear-velocity model of the crust and upper mantle, *Geophys. J. Int.*, *151*, 88-105.
- Shaw, D. M., J. J. Cramer, M. D. Higgins, and M. G. Truscott (1986), Composition of the Canadian Precambrian shield and the continental crust of the Earth, in *The Nature of the Lower Continental Crust*, edited by J. B. Dawson et al., pp. 257-282, Geol. Soc. of London, London, U. K.
- Taylor, S. R., and S. M. McLennan (1985), *The Continental Crust: Its Composition and Evolution*, Blackwell, Oxford, U. K.
- Taylor, S. R., and S. M. McLennan (1995), The geochemical evolution of the continental crust, *Rev. Geophys.*, *33*(2), 241-265.
- Tondi, R., R. Schivardi, I. Molinari, and A. Morelli (2012), Upper mantle structure below the European continent: Constraints from surface-wave tomography and GRACE satellite gravity data, *J. Geophys. Res.*, *117*, B09401, doi:10.1029/2012JB009149.
- Uieda, L., E. P. Bomfim, C. Braitenberg, and E. Molina (2011), Optimal forward calculation method of the Marussi tensor due to a geologic structure at GOCE height, Proc. of '4th International GOCE User Workshop', Munich, Germany.
- van der Meijde, M., R. Pail, R. Bingham, and R. Floberghagen (2015), GOCE data, models, and applications: A review, *Int. J. Appl. Earth Obs.*, *35*, 4-15.
- Vitovtova, V. M., V. M. Shmonov, and A. V. Zharikov (2014), The porosity trend and pore sizes of the rocks in the continental crust of the Earth: Evidence from experimental data on permeability, *Izv. Phys. Solid Earth*, *50*(5), 593-602.
- Wyllie, M. R. J., A. R. Gregory, and G. H. F. Gardner (1958), An experimental investigation of factors affecting elastic wave velocities in porous media, *Geophysics*, *23*(3), 459-493.
- Youssef, M., H. Thybo, I. M. Artemieva, and A. Levander (2013), Moho depth and crustal composition in Southern Africa, *Tectonophysics*, *609*, 267-287.
- Zandt, G., and C. J. Ammon (1995), Continental crust composition constrained by measurements of crustal Poisson's ratio, *Nature*, *374*, 152-154.